ACCURACY ASSESSMENT OF BURNED AREA PRODUCTS IN THE ORINOCO BASIN

Jesús Anaya, Profesor Asociado
Universidad de Medellín
Carrera 87 No.30-65, Medellín, Colombia, S.A
janaya@udem.edu.co

Emilio Chuvieco, Catedrático
Universidad de Alcalá
Calle Colegios 2, 28801, Alcalá de Henares, Madrid, España
emilio.chuvieco@uah.es

ABSTRACT

Burned area products derived from satellite images are used as input to determine biomass burning emissions. Appropriate assessment of the accuracy of burned area products is required to assess reliable emissions. This document provides validation results for four burned area products: GlobCarbon, MCD45, L3JRC and AQS. The study area is at the northern South American savannas along the Orinoco River since there is a rapid conversion of Amazonian forest to cattle pasture. A validation method was applied from 2001 to 2007 based on the comparison of commission and omission errors from 20 confusion matrixes with their respective efficient solution. Efficient solutions were determined using the "Pareto Boundary". This method allows estimating the potential for improving burned area algorithms as well as evaluating the effect of pixel size on accuracy. A landscape metric was used to analyze the weight of the fragments' distribution on global accuracy. It was found that all products underestimate burned area and that an increase in pixel size or border density results in larger burned area estimate errors.

INTRODUCTION

Biomass burning has a large variety of impacts on the local, regional and global scale. Even though fire has been recognized as a natural process in several ecosystems, it has also been associated with negative effects on soil, water, vegetation and the atmosphere. At a local scale, it has been found that fire modifies aspects of the hydrological cycle as run-off and transpiration, increases soil erosion and alters vegetation succession. At a regional scale there is a concern for nations to meet the Kyoto protocol, to achieve sustainability of forest ecosystems, and to reduce large biomass burning emissions. Finally, at a global scale there is a growing concern of biomass burning in relation to global warming, greenhouse emissions, changes of the properties and composition of the atmosphere and changes of solar radiation budgets on the earth surface.

Tropical forests are considered a large carbon pool at regional and global levels; however, nowadays these forests are undergoing deforestation at unprecedented rates. Fire in the tropics is related to agricultural activities such as, cattle grazing and land use change (forest to agriculture), with more fires occurring due to temperature increase and accelerated land use change (Cardoso et al. 2003). Biomass burning is induced during the dry season and its negative effects are worsened with natural phenomena like El Niño ENSO (Levine et al. 1999).

Remote sensing techniques are used to monitor fires and burned areas. There is a large decrease in reflectance after the occurrence of fires in the vegetation coverage. This change in reflectance is used to classify satellite images in burned and non-burned pixels. This type of map is commonly referred as "burned area product". Considerable uncertainties remain in the quantification of burned area, particularly in the tropics where burned areas are usually small (less 1 km^2) and therefore remain undetected (Schultz et al. 2008). This paper focuses on the uncertainty caused by burned area products developed at global and regional levels.

In the year 2000, the first two products of burned area were developed at a global scale, known as GBA2000 - Global Burnt Areas- (Tansey et al. 2004) and GlobScar (Simon et al. 2004). The goal of these two maps was to create homogeneous information at a global scale with a standard methodology and a spatial resolution of 1000 m (Hoelzemann et al. 2004). At the moment, the burned area maps most frequently used are, L3JRC http://www-tem.jrc.it and GlobCarbon http://www.geosuccess.net, which are improved versions of GBA2000 and GlobScar projects, respectively. Another product designed at a global scale is the MCD45, based on data from the Moderate

Resolution Imaging Spectroradiometer (MODIS) surface reflectance time series. This product has created high expectations due to its 500 m spatial resolution. At the regional level, two products are of importance to the study area. One is elaborated by Chuvieco et al. (2008) and is derived from the MODIS 32 day composite data and the other AQS (Area Quemada Sudamerica), is derived from the MODIS 16 day composites MCD43 (Opazo and Chuvieco, 2009).

The improvements made on burned area products cannot avoid the pitfalls of satellite derived information, such as: low spatial resolution, confusion with non-vegetated coverage (dark soils, shadows, water bodies); complex configuration of burned areas within the landscape (too small or highly fragmented) (Smith et al. 2003, Silva et al. 2005); and limitations related to gases like clouds or smoke plumes. In addition, several factors contribute to the variation of the signal, such as: type of burned coverage, burning efficiency, fire severity, fraction of material exposed to fire, and post fire physical evolution of the surface (Ward et al. 1996, Miller and Yool 2002, Roy and Landmann 2005).

The confusion matrix method has been commonly used since the 1980's to validate thematic maps (Congalton 2001) including burned area maps (Morisette et al. 2002, Quintano et al. 2002, Roman-Cuesta et al. 2005). The confusion matrix is a square matrix that indicates the number of pixels assigned to a particular class in relation to the information considered as field work, i.e. reference data. Reference information is usually located at the columns and the map to be validated at the rows. For this reason, all values except the diagonal are errors, while the diagonal represents the agreements between true data and modeled data.

The goal of this study is to assess the effect of fragmentation on the accuracy of burned area maps, evaluate the differences in accuracy related to pixel size and determine the potential of burned area algorithms for improvement.

METHODOLOGY

The study area is located in the northern savannas of South America along the tributaries of the Orinoco River Fig. 1. The area is highly prone to fires due to pasture burning and forest clearing. In fact, Colombia and Venezuela have been found to be among the most affected countries in relation to their territory (Chuvieco et al. 2008). Increasing deforestation along the Amazon forest, due to the growing need of cropping and grazing lands, has created a broad mosaic of burned areas. Temporal priority was given to the dry season months of January, February and March.

Figure 1. Study area and WRS (path-row) location of Landsat images at the areas with largest biomass burning between Colombia and Venezuela. P004r056 (two images), P005R056 (three images), P006r058 (one image), P005R057 (one image), P184R094 (one image -CBERS bold-).

The validation process requires field data, a map to be evaluated and a validation method such as the confusion matrix. A proxy for field data is the interpretation of high resolution satellite images. There are two reasons for using this proxy. First, it is impossible to cover the geographic extent of a regional or global product with field work. Second, the charcoal signal commonly has a short duration and therefore, available archive data is the only means by which one can determine individual burned patches (Boschetti et al. 2006). Landsat images have been successfully used in previous studies as a proxy for burned areas field work because it has adequate spatial and spectral resolution (Roy et al. 2005, Boschetti et al. 2006, Chuvieco et al. 2008)

Reference Information

Satellite images from the Landsat TM/ETM+ and CBERS CCD were interpreted and classified in a dichotomic way: burned and non-burned. Training regions were drawn over the images, assigning individual training regions to different tones of burned area. Once all different tones of burned areas were included, a maximum likelihood classification was applied. A supervised classification in ETM+ images obtained after the 14th of July 2003 cannot be performed due to the scan line corrector failure (SLC-off). For this reason, visual interpretation was used for SLC-off Landsat images. Reference images for validation were carefully selected, only those images with large amounts of burned areas and free from clouds were chosen. Images at the same location within the same dry season were disregarded. It was impossible to select reference images through a statistical design following these constraints. However, selected scenes are representative of the region of interest, covering savanna, primary forest and secondary forest. Seven Landsat images and one CBERS image were classified using supervised classification.

Products to Validate

A total of four products of burned area are validated in different dates from 2001 to 2007: 1) GlobCarbon, is the result of the GlobScar project that started in 2001 with ATSR (Along Track Scanning Radiometer) (Simon et al. 2004); 2) GBA 2000, based on VEGETATION instrument onboard SPOT satellite (Tansey et al. 2007); 3) MCD45,

this is the MODIS burned area product Roy et al. (2005); and 4) the *Área Quemada para Sudamérica* (AQS) based on non-standard 32-days MCD45 Modis composites (Opazo and Chuvieco 2009)

Validation Methods

Burned area product validation was performed following the confusion matrix. This method allows comparing a field truth map with the map to be evaluated. In order to do so, all spatial information was projected to UTM18-WGS84, assuring that map extent and pixel size were the same for reference maps and maps to be validated. The confusion matrix allows determining global accuracy, omission errors (Oe) and commission errors (Ce). Aside from the confusion matrix, the "Pareto Boundary" described by Boschetti et al. (2004b), was calculated in order to determine the effect of pixel size 500 m (MCD45) and 1000 m (AQS, L3JRC and GlobCarbon) on map accuracy.

The Pareto Boundary was defined by a set of points that belongs to the boundary and drawn in a two dimension (Oe/Ce) coordinate system. To calculate each point, a low resolution grid of 500 m or 1000 m must be overlaid on to the high resolution image (reference), and then the amount of burned area of the high resolution image is measured as the percentage for each pixel of the low resolution map (Fig. 2). At this point each pixel of the low resolution map has a percentage value between 0 and 100, representing the amount of burned area at the high resolution map for the same area. If only those pixels with a 100% burned of the low resolution map are considered as burned, the commission error is zero but the omission error is extremely high. If on the other hand, a pixel is considered as burned at any percentage of burned area, the omission error (Oe) is zero, but the commission error (Ce) is extremely high. Intermediate points could be calculated at different percentages of burned area on the low resolution map in order to get more (Oe/Ce) coordinates. In other words, the set of coordinates (Oe/Ce) belonging to the Pareto boundary is built by changing the percentage threshold in which a cell would be considered as burned. Five thresholds (90-100%, 75-100%, 50-100%, 25-100%, 0-100%) were used for each pair of reference image and low resolution map to describe the Pareto boundary.

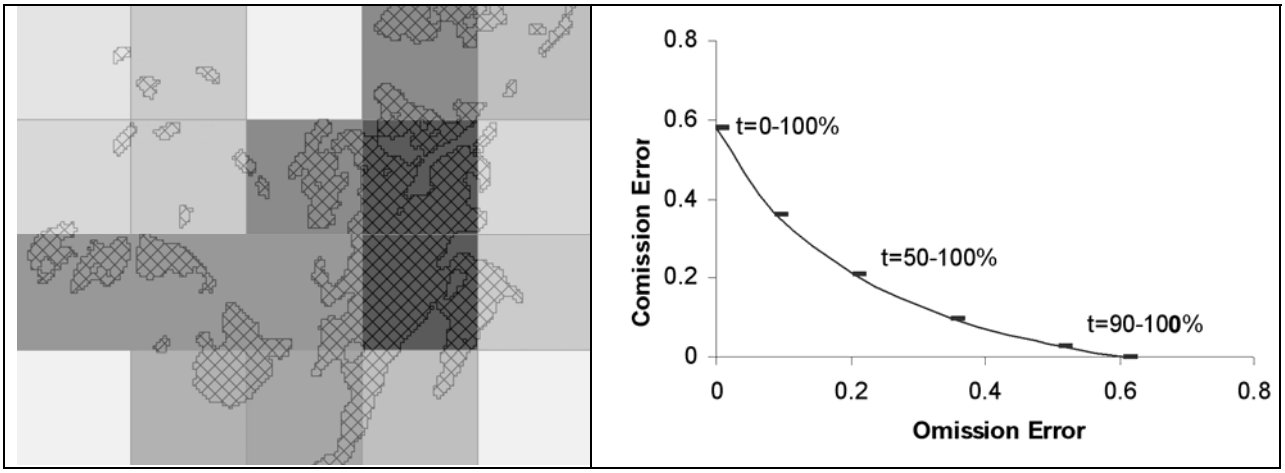

Figure 2. Subset of a low resolution grid overlaid on a high resolution image (left) and Pareto Boundary (Right). The percentage of burned area on the low resolution cells changes from non-burned cell (white, 0%) to completely burned cell (black, 100%). The selection of thresholds results in coordinate pairs of Omission and Commission errors (Oe/Ce).

In addition to the Pareto boundary, which mainly describes the effect of the pixel size, a landscape metric known as edge density (ED) was calculated to describe the effect of fragmentation. This metric is based on area and perimeter of burned areas (Fassnacht et al. 2006, Miettinen 2007), and is a measure of the complexity and shape of the polygons. It was calculated as a fraction of the total perimeter to the total area:

$$ED = \Sigma(BAP)/\Sigma(BA)$$

where;
ED (m/ha): Edge Density
BAP (m): Perimeter for each burned area
BA (ha): Surface for each burned area.

The burned class defined in the reference images was vectorized in order to get perimeter and surface for each burned area. Large values of Edge Density indicate complex shapes and long borders, while low values indicate simple and compact shapes (Silva et al. 2005).

RESULTS

Table 1 presents the results of 20 confusion matrixes calculated between the reference images and each of the products evaluated. In general, global accuracy is around 90% due to the large amount of agreements between non-burned pixels. Burned area omission errors are those affecting global accuracy the most. There is a tendency of omission errors (mean 0.44) to be larger than commission errors (0.38), which translates into an underestimation of total burned area.

Table 1. Pair of coordinates Oe/Ce for Burned Area of a total of 20 confusion matrixes. Each matrix is identified by its date which corresponds to a Landsat ETM+ and CBERS reference images.

Omission Error	Commission Error		Overall Accuracy	Kappa coefficient	Image ID Path/row/yr/month/day
		AQS			
46.1	25.5		95.3	0.60	P006R05820040201
72.6	60.6		71.6	0.15	P005R05620040210
84.8	20.4		93.7	0.23	P005R05620051229
		GlobCarbon			
92.6	85		99.5	0.09	P004R05620010109
54.2	53.7		90.8	0.41	P005R05620010201
45.9	17.2		95.9	0.63	P006R05820040201
70.2	66.3		68.1	0.11	P005R05620040210
		L3JRC			
68	73.6		96.8	0.27	P004R05620010109
55.6	47		91.9	0.44	P005R05620010201
52.5	11.4		95.8	0.59	P006R05820040201
78.7	63.7		71.3	0.1	P005R05620040210
70.6	28.1		94.2	0.39	P005R05620051229
54.5	59.3		88.5	0.36	P184R09420070206
65.4	30.1		89.9	0.41	P004R05620070211
77.5	24.5		88.2	0.30	P005R05720070218
		MCD45			
71.3	53.4		97.9	0.34	P004R05620010109
40.0	49.2		91.6	0.50	P005R05620010201
54.8	51.4		90.2	0.41	P184R09420070206
66.2	29.2		89.9	0.41	P004R05620070211
77.9	20.3		88.4	0.30	P005R05720070218

Although there is a pattern towards larger omission errors (Fig. 3) there is also a large dispersion of Oe/Ce values. Dispersion is reduced drastically when Oe/Ce values are considered by scene as shown by the ellipses, i.e. algorithms behave similarly within scenes but are highly variable among scenes. In order to find the reliability of the burned area products algorithms and to assess the effect of the pixel size, the Pareto boundary method (from now referred to as efficient solution) was applied.

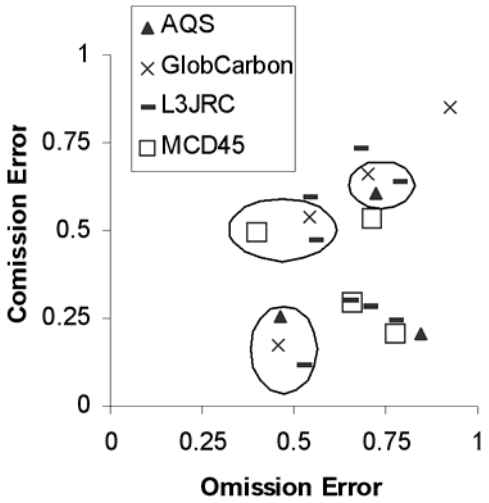

Figure 3. Pairs of Omission and Comission errors calculated using a confusion matrix; ellipses include Oe/Ce of individual images.

The area under the efficient solution curve is defined by Boschetti (2004) as the unreachable region, there is no combination of Oe/Ce values for a given pixel size that could result in lower values. Thus, the Oe/Ce values from a confusion matrix are above the curve and its distance represents the potential of the burned area algorithm to be improved. Four out of thirteen calculated efficient solutions are shown (Fig. 4). Each combination of reference image with low resolution images results in a different boundary. It was found that for the same reference image, the area under the efficient solution is always lower for a 500 m pixel than for a 1000 m pixel. No major differences were found between Oe/Ce values and efficient solutions, which in turn indicate similar inaccuracy due to the algorithms disregarding pixel size.

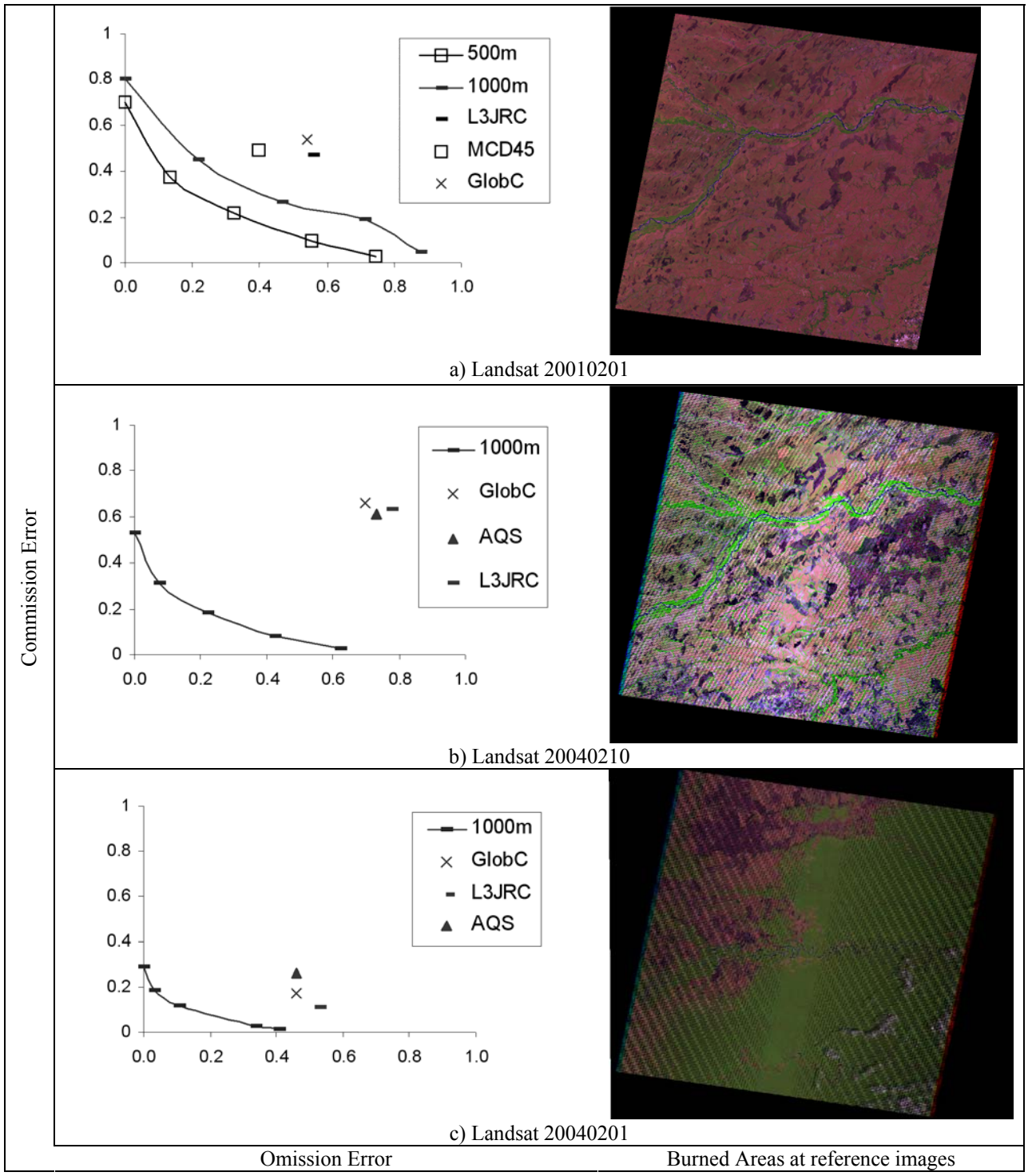

Figure. 4. Efficient solutions at different thresholds (t) for two different pixel sizes: 500 m and 1000 m (a), and 1000 m only (b,c). Points are confusion matrix commission and omission errors for MCD45, GlobCarbon, L3JRC and AQS.

No major differences were found when evaluating the distances between Oe/Ce values and efficient solutions per each scene. This might be an indication of similar disadvantages of the algorithms disregarding pixel size. However, large differences were found among scenes. Figure (4b) shows the Oe/Ce values are far from the curve, indicating poor performance, in contrast, the pairs of Oe/Ce coordinates on Figure (4a) are close to its maximum accuracy, indicating the high quality of the algorithm.

The area under the efficient solution curve is an indication of the accuracy that a burned area algorithm can achieve. Since the efficient solution is sensitive to the size of the pixel it should also be affected by the landscape distribution of the burned area fragments. A metric of landscape ecology was applied to each reference image scene to evaluate the effect of fragmentation on the efficient solution. The metric was calculated using the vectorized area and perimeter of the reference image polygons. There are a total of eight curves, one for each reference image calculated with a grid of 1000 m. Figure 5 presents a series of efficient solutions, each related to its respective edge density (ED) metric. The metric value increases as the area under the curve increases, which at the same time increases burned area estimation inaccuracy.

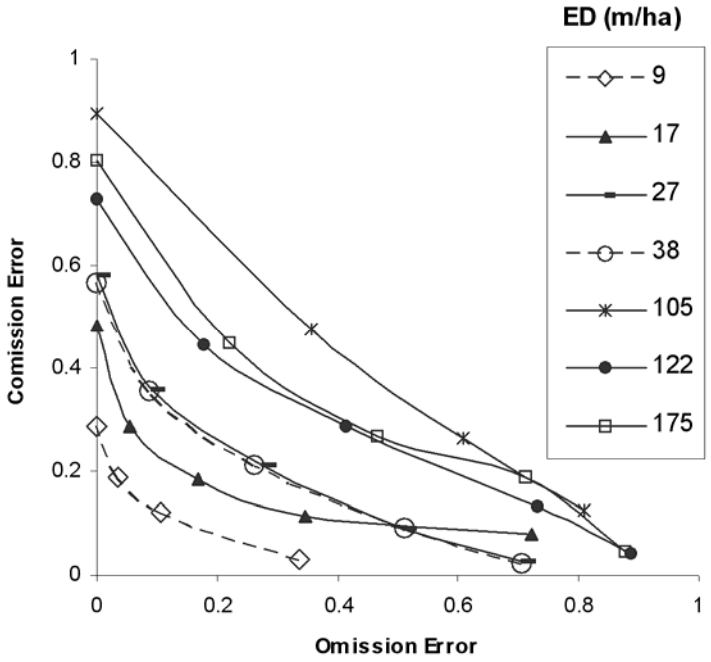

Figure 5. Efficient solutions curves calculated for each high resolution scene and a 1000 m grid cell size with their respective Edge Density (ED) metric.

DISCUSSION AND CONCLUSIONS

A major challenge when validating burned area products is to achieve the largest temporal coherence between the date of the high resolution images and the product to be validated. This is only possible if both data sources have the day of detection in each pixel, which evidently was not the case for the high resolution images, where the only date available is the one when the image was taken. Fortunately, MCD45, L3JRC and GlobCarbon provide the day of detection per pixel allowing validation of burned pixels previous to the date of the high resolution image. This is not the case for AQS, which can only provide the date of the end of the 16-day composite.

As discussed above, validation was made depending on the burned area product and the reference image availability. It was found that AQS has the largest omission errors and lower commission errors; L3JRC and GlobCarbon presented similar omission errors but commission errors are lower in L3JRC, and finally, MCD45 had the lowest omission errors with commission errors slightly above those from AQS. These results indicate that the best burned area product is MCD45, but L3JRC is the best of the 1000 m spatial resolution products. The availability of high resolution images does not permit more conclusive results. Although not statistically valid, similar tendencies are likely to appear if more data for validation were available.

It was found, for all the evaluated products, that omission errors are larger than commission errors for the study area, similar to those found by Tansey et.al (2007) for Africa. Omission errors in burned area are the result of an underestimation at this class and it could be argued that it is compensated by commission errors. The main reason for larger omission than commission errors, based on our observations, is related to the surface area of the burned fragments disregarding burned biomass class: small areas are constantly underdetected. It is possible that the underdection is only related to sensor constraints or to undocumented contextual procedures. The latter not only aggregates pixels, but also eliminates single pixels in order to avoid the salt and pepper effect. The underdetection issue is more important when located at forests, usually having few hectares, but producing the largest and long lasting greenhouse emissions.

The efficient solution has been shown to be sensitive to both pixel size and the burned area distribution in the landscape. The edge density landscape metric is easy to calculate and its simplicity allows for a straightforward interpretation. Here, it was shown that an increase in pixel size as well as an increase of fragmentation of burned areas results in larger omission and commission errors. In contrast, the distance between the Oe/Ce values with their respective efficient solutions is quite similar among products. This shows that the size of the pixel of the burned area product is more important than differences among algorithms.

When estimating burned areas or emissions, Hoelzemann (2004) and Roy (2005b) concluded that different satellite information should be considered. In this sense and as an alternative to omission in forests Boschetti et al. (2004a), found that Fire Active Data like World Fire Atlas (WFA) could be used as a complement for burned area products. Further research on the detection of both small burned areas and understory burning is required.

REFERENCES

Boschetti, L., P.A. Brivio, H. Eva, J. Gallego, A. Baraldi, and J. M. Gregoire, 2006. A Sampling Method for the Restrospective Validation of Global Burned Area Products, *IEEE Transactions on Geoscience and Remote Sensing*, 44:1765-1772.

Boschetti, L., H.D. Eva, P.A. Brivio, and J.M. Gregoire, 2004a. Lessons to be learned from the comparison of three satellite-derived biomass burning products, Geophysical research letters 31(L21501):doi:10.1029/2004GL021229.

Boschetti, L., S.P. Flasse, and P.A. Brivio, 2004b. Analysis of the conflict between omission and commission in low spatial resolution dichotomic thematic products: The Pareto Boundary, *Remote Sensing of Environment*, 91:280-292.

Cardoso, M.F., G.C. Hurtt, B. Moore III, C.A. Nobre, and E.M. Prins, 2003. Projecting future fire activity in Amazonia, *Global Change Biology*, 9:656-669.

Congalton, R.G., 2001. Accuray assessment and validation of remotely sensed and other spatial information, *International Journal of Wildland Fire*, 10:321-328.

Chuvieco, E., S. Opazo, W. Sione, H. Del Valle, J. Anaya, C. Di Bella, I. Cruz, L. Manzo, G. Lopez, N. Mari, F. Gonzalez, F. Morelli, A. Setzer, I. Csiszar, A. Karpandegui, A. Bastarrika, and R. Libonari, 2008. *Global Burned Land Estimation in Latin America using MODIS Composite Data. Ecological Applications*, 18:64-79.

Fassnacht, K., W. Cohen, and T. A. Spies, 2006. Key issues in making and using satellite-based maps in ecology: A primer, *Forest Ecology and Management*, 222:167-181.

Hoelzemann, J.J., M.G. Schultz, G.P. Brasseur, and C. Granier, 2004. Global Wildland Fire Emission Model (GWEM): Evaluating the use of global area burnt satellite data, *Journal of Geophysical Research*, 109:doi:10.1029/2003JD003666.

Levine, J.S., T. Bobbe, N. Ray, and R.G. Witt, 1999. Wildland Fires and the Environment: A Global Synthesis. Pages 1-52 in *UNEP/DEIAEW/TR.99-1.*, editor.

Miettinen, J., 2007. Burnt Area Mapping in Insular Southeast Asia Using Medium Resolution Satellite Imagery, University of Helsinki, Helsinki.

Miller, J.D. and S.R. Yool, 2002. Mapping forest post-fire canopy consumption in several overstory types using multi-tempora Landsat TM and ETM data, *Remote Sensing of Environment*, 82:481-496.

Morisette, J.T., J.L. Privette, and C.O. Justice, 2002. A framework for the validation of MODIS Land products, *Remote Sensing of Environment*, 83:77-96.

Opazo, S. and E. Chuvieco, 2009. Cartografía de áreas quemadas en Sudamérica: Detección de píxeles semilla, *Revista de Teledetección*, 32:50-71.

Quintano, C., A. Fenández, J.A. Delgado de la Mata, and Y.E. Shimbukuro, 2002. Determination of spectral mixture analysis validity for estimating burned area using AVHRR data and multitemporal analysis, pp. 1-10 in *Forest Fire Research & Wildland Fire Safety*, Millpress, Rotterdam.

Roman-Cuesta, R.M., J. Retana, M. Gracia, and R. Rodriguez, 2005. A quantitative comparison of methods for classifying burned area with LISS-III imagery, *International Journal of Remote Sensing*, 26:1979-2003.

Roy, D. and T. Landmann, 2005. Characterizing the surface heterogeneity of fire effects using multi-temporal reflective wavelength data, *International Journal of Remote Sensing*, 26:4179-4218.

Roy, D.P., Y. Jin, P.E. Lewis, and C.O. Justice, 2005. Prototyping a global algorithm for systematic fire-affected area mapping using MODIS time series data, *Remote Sensing of Environment*, 97:137-162.

Schultz, M.G., A. Heil, J.J. Hoelzemann, A. Spessa, K. Thonicke, J. G. Goldammer, A.C. Held, J.M. C. Pereira, and M. van het Bolscher, 2008. Global wildland fire emissions from 1960 to 2000, Gl*obal Biogeochemical Cycles*, 22(GB2002):doi:10.1029/2007GB003031.

Silva, J.M.N., A.C.L. Sá, and J.M.C. Pereira, 2005. Comparison of burned area estimates derived from SPOT-VEGETATION and Landsat ETM+ data in Africa: Influence of spatial pattern and vegetation type, *Remote Sensing of Environment*, 96:188-201.

Simon, M., S. Plummer, F. Fierens, J.J. Hoelzemann, and O. Arino, 2004. Burnt area detection at global scale using ATSR-2: The GLOBSCAR products and their qualification, *Journal of Geophysical Research*, 109(D14S02):doi:10.1029/2003JD003622.

Smith, J.H., S.V. Stehman, J.D. Wickham, and L. Yang, 2003. Effects of landscape characteristics on land-cover class accuracy, *Remote Sensing of Environment*, 84:342-349.

Tansey, K., J.-M. Grégoire, J.M.C. Pereira, P. Defourny, R. Leigh, J.-F. Pekel, A. Barros, J.N.M. Silva, E. van Bogaert, E. Bartholomé, and S. Bontemps, 2007. L3JRC - A global, multi-year (2000-2007) burnt area product (1 km resolution and daily time steps), in *Remote Sensing and Photogrammetry Society Annual Conference 2007*, Newcastle upon Tyne, UK.

Tansey, K., J.M. Gregoire, E. Binaghi, L. Boschetti, P.A. Brivio, D. Ershov, S.P. Flasse, R. Fraser, D. Graetz, M. Maggi, P. Peduzzi, J.M.C. Pereira, J.N.M. Silva, A. Sousa, and D. Stroppiana, 2004. A Global inventory of burned areas at 1 km resolution for the year 2000 derived from SPOT vegetation data, *Climatic Change*, 67:345-377.

Ward, D., W.M. Hao, R.A. Susott, and R.E. Babbitt, 1996. Effect of fuel composition on combustion efficiency and emission factors for African savanna ecosystems, *Journal of Geophysical Research*, 101:23,569-523,576.